Copy 5
RM E56L06

C.1

NACA RM E56L06

NACA

RESEARCH MEMORANDUM

EXPERIMENTAL INVESTIGATION OF A 0.4 HUB-TIP DIAMETER RATIO AXIAL-FLOW COMPRESSOR INLET STAGE AT TRANSONIC INLET RELATIVE MACH NUMBERS

IV - PERFORMANCE OF TAPERED-TIP ROTOR CONFIGURATION WITH RESET BLADE ANGLES

By John C. Montgomery and Frederick Glaser

Lewis Flight Propulsion Laboratory
Cleveland, Ohio

NATIONAL ADVISORY COMMITTEE
FOR AERONAUTICS

WASHINGTON
February 28, 1957

NATIONAL ADVISORY COMMITTEE FOR AERONAUTICS

RESEARCH MEMORANDUM

EXPERIMENTAL INVESTIGATION OF A 0.4 HUB-TIP DIAMETER RATIO AXIAL-FLOW COMPRESSOR INLET STAGE AT TRANSONIC INLET RELATIVE MACH NUMBERS

IV - PERFORMANCE OF TAPERED-TIP ROTOR CONFIGURATION WITH RESET BLADE ANGLES

By John C. Montgomery and Frederick Glaser

SUMMARY

The blades of the tapered-tip 0.4 hub-tip diameter ratio transonic rotor were reset $7\frac{1}{2}^{\circ}$ in the rotor disk and twisted from 0° at the mean-radius section to $4\frac{1}{2}^{\circ}$ at the tip to increase the specific weight flow approximately 10 percent to 36.3 pounds per second per square foot of frontal area.

At design speed, the reset rotor produced the design pressure ratio of 1.38 at a specific weight flow of 35.6 pounds per second per square foot at an efficiency of 0.91. Peak efficiency and maximum pressure ratio at design speed were 0.925 and 1.44, respectively. Peak efficiencies at 60, 80, and 115 percent of design speed were 0.91, 0.94, and 0.87, respectively.

The radial selection of the blade-element parameters was good so that high compressor efficiency was obtained but at a weight flow below the design value.

The increased values of minimum-loss incidence angles obtained at the rotor hub section (approximately 4° at design speed) are compared with previously published curves relating minimum-loss incidence to cascade rules and to an empirical choke-incidence-angle rule.

INTRODUCTION

The advantages of transonic axial-flow compressor stages are pointed out in previous publications (e.g., refs. 1 to 3). In each of these

references, axial-flow rotors operating in the transonic region were designed and tested in order to further the knowledge on the performance of transonic rotors over a range of flow conditions.

In some cases, such as in references 4 and 5, information on new areas of flow conditions were obtained by merely resetting the rotor blades or modifying an existing design.

In reference 4, the effect of blade loading at the rotor-blade tip section was investigated by modifying the 0.4 hub-tip diameter ratio transonic compressor of reference 3. The compressor was modified by employing an insert along the outer-casing wall and tapering the insert inward across the rotor-blade row; the blades were unchanged except that the blade tips were machined down to conform to the new outer-casing contour. With the modification the axial velocity at the rotor outlet was increased for a given inlet condition, and therefore the blade loading or the blade diffusion factor was reduced. The maximum reduction in the blade loading occurred at the rotor tip section because the effect of the insert and the outer-wall curvature increased the axial velocity the most at that section. At design speed the modification of the compressor increased the peak efficiency of the rotor tip section from 0.80 to 0.92, approximately doubled the weight-flow range, and decreased the maximum weight flow approximately 3 percent.

From the results of reference 4 it was determined feasible to increase the weight flow of the 0.4 hub-tip diameter ratio transonic rotor with the decreased tip loading by resetting the rotor-blade angles. The blades of the transonic rotor of reference 4 were reset in order to (1) increase the specific weight flow approximately 10 percent and (2) obtain additional information on the performance of transonic rotor blades (hub section) where the relative outlet air is turned past the axial direction. To date, limited information (ref. 6) is available on the performance of transonic rotor blades turning the relative air past the axial direction. Consequently, the blades used in the investigation of reference 4 were both reset and twisted to handle an increase of weight flow of approximately 10 percent. The reset tapered-tip rotor was run over a range of weight flows at speeds from 60 to 115 percent of design speed.

APPARATUS AND PROCEDURE

Rotor Design and Modification

The detail design of the original 0.4 hub-tip diameter ratio transonic rotor and the insert employed to taper the rotor tip are presented in references 3 and 4, respectively. In brief, the original rotor was designed to produce a pressure ratio of 1.35 at a corrected specific

weight flow of 34.9 pounds per second per square foot of frontal area. The diameter of the rotor was 14 inches and the design tip speed was 1000 feet per second. The rotor was designed for axial air inlet and for constant energy addition along the radius. For the tapered-tip configuration (ref. 4), the rotor was modified by employing an insert along the outer-casing wall and tapering the insert inward across the rotor-blade row. The blades for the tapered-tip configuration were unchanged except that the tips were machined down to fit the new outer-casing contour. As pointed out in reference 4, the tapered-tip modification of the 0.4 hub-tip diameter ratio transonic rotor increased the rotor-blade tip-section efficiency at design speed from 0.80 to 0.92, increased the over-all efficiency from 0.93 to 0.95, doubled the weight-flow range, and decreased the maximum flow capacity approximately 3 percent.

In order to calculate the blade-setting-angle changes required to increase the weight flow to 36.3 pounds per second per square foot, an analysis of the design-speed performance data of the 0.4 hub-tip diameter ratio rotor (refs. 4 and 7) was made. The data showed that the minimum-loss incidence angle varied from approximately 4° at the tip section (10 percent of passage height from the outer wall) to 8° at the hub section (10 percent of the passage height from the inner wall), as shown in figure 1. Hereinafter, the terms tip and hub sections will be used to refer to the blade sections 10 percent of the passage height from the annulus walls. Included in figure 1 is the incidence-angle variation at the near over-all peak-efficiency weight flow of 32.50 pounds per second per square foot for the tapered-tip rotor configuration. The tapered-tip rotor blade was well matched and the incidence angles were within 1° of minimum-loss incidence angle at all radii for the peak-efficiency weight flow.

By using the same velocity distribution at the rotor inlet as was obtained for the tapered-tip rotor configuration, the incidence-angle variation for a weight flow of 36.3 pounds per second per square foot was calculated and is included in figure 1. In order to have the rotor operate at the increased weight flow, it was necessary to reset the rotor blades so that the new incidence angles would match the minimum-loss incidence-angle values anticipated for the reset blade at the increased flow. The design rules of reference 8 indicated that the values of minimum-loss incidence angles obtained for the tapered-tip rotor would not increase for the reset blades at the increased weight flow. At the hub section, however, where the blade setting angle was to be reduced from 14.2° to 8.1°, the minimum-loss incidence angle was arbitrarily increased from 8° to 9.5° (the blade setting angle reduced to 6.6°) in anticipation of the possibility of the rotor choking at that section. This arbitrary increase of the incidence angle was made because the blade setting angle at the hub section was lower than any of the blade setting angles of the reference rotors on which the design rule of reference 8 was based.

By using the assumed minimum-loss incidence angle of 9.5° at the hub section and the minimum-loss incidence angles of reference 4 at the other radii, the required blade-setting-angle changes for the increased flow varied from 7.6° at the hub section to 3.8° at the tip section, as shown in figure 1. The required change of the blade setting angle is plotted against percent of passage height in figure 2. In order to approximate the calculated variation in the blade setting angles, it was necessary to reset the blades 7.5° in the rotor disk and to untwist the blades 4.5° at the rotor tip while holding the blades fixed along and below the midpassage streamline. Because of mechanical limitations, it was necessary to relieve the blades a short distance below the mean-section streamline to avoid a sharp bend. For this reason, the change in the blade setting angle in the vicinity of the mean-section streamline was indeterminate. The resultant variation in the actual blade setting angles obtained from resetting and untwisting the blades is shown by the solid curve in figure 2. The variation of the actual blade setting angles near the midpassage is shown as a dotted segment because of the mechanical limitations stated.

Simple radial equilibrium calculations $\left(\frac{1}{\rho}\frac{dp}{dr} = \frac{V_\theta^2}{r}\right)$ neglecting the effect of streamline curvature at the rotor outlet were performed to determine the resultant rotor outlet conditions. Values for total-pressure-loss coefficients and deviation angles were obtained from references 4 and 7 at the minimum-loss incidence angles. The calculations were carried out for five radial blade-element stations spaced at 10, 30, 50, 70, and 90 percent of the passage height from the outer wall. In solving the simple radial equilibrium equation, the value of the static pressure was assumed at the rotor tip and its radial variation was calculated. The magnitude of the assumed static pressure at the rotor tip was varied until continuity through the rotor was satisfied. The simple radial equilibrium calculations showed that the resultant pressure ratio and rotor tip diffusion factor would be approximately 1.38 and 0.19, respectively.

With the reset and twisted blades installed in the compressor, the tip clearance increased from approximately 0.030 inch (clearance of tapered-tip configuration, ref. 4) to 0.045 inch at the rotor-blade leading and trailing edges.

For the tapered-tip reset rotor configuration the annulus area downstream of the rotor outlet measuring station was enlarged at both the inner and outer walls (fig. 3) to accomodate the increase in weight flow.

Compressor Installation and Instrumentation

The compressor installation and instrumentation are the same as those described in reference 4. The axial measuring stations used to

determine the rotor performance were located 1/2 inch upstream and 1/2 inch downstream of the rotor leading and trailing edges at the hub, respectively. At the rotor inlet, total pressure, static pressure, and air angle were measured at the five major radial stations located at 10, 30, 50, 70, and 90 percent of the passage height from the outer wall. Static pressure was also measured at the outer and inner walls. Additional measurements of angle and total pressure were made at 3, 5, and 7 percent of the passage height from both the outer and inner walls.

4207

Total pressure, total temperature, and air angle at the rotor outlet were measured and recorded continually by an automatic recorder as the combination probe was transversed radially across the passage. Static pressure was measured at the five major radial stations (10, 30, 50, 70, and 90 percent of passage height from the outer wall) and at both the inner and outer walls.

In references 3, 4, and 7 the performance of the 0.4 hub-tip diameter ratio rotor was plotted against the weight flow measured by the inlet orifice. In this report, however, the performance of the 0.4 hub-tip diameter ratio rotor is plotted against the integrated weight flow measured at the rotor inlet. This change in the reference weight flow was made because more consistent results were obtained with the inlet integrated weight flow. Therefore, the weight-flow values presented in this report for the tapered-tip rotor differ somewhat from the weight-flow values presented in reference 4 for the same rotor.

Procedure

Data were obtained for corrected speeds of 60, 80, 100, and 115 percent design speed. For each speed the weight flow was varied from open throttle to a value where blade vibration was indicated by the magnetic plug-type pickup (ref. 4).

At each weight-flow point, complete surveys were made at the rotor inlet and rotor outlet axial measuring stations. The over-all performance of the rotor is presented as the arithmetically averaged rather than the mass-averaged values so as to be consistent with the data presented in reference 4. The blade-element performance parameters are presented at five major radial stations located at 10, 30, 50, 70, and 90 percent of the passage height from the outer wall.

The symbols used herein are included in the appendix.

RESULTS

Rotor Over-All Performance

The over-all performance of the reset tapered-tip rotor is presented in figure 4 together with the over-all performance of the tapered-tip rotor of reference 4. The weight-flow values presented in figure 4 are the integrated weight-flow values measured at the rotor inlet and, therefore, for the case of the tapered rotor, differ somewhat from the values presented in reference 4 as pointed out in the section Compressor Installation and Instrumentation.

The reset tapered-tip rotor produced the design pressure ratio of 1.38 at a specific weight flow of 35.6 pounds per second per square foot at an efficiency of 0.91. As shown by figure 4, the weight flow was 0.7 pound less than the design value of 36.3 pounds per second per square foot. Although the efficiency at the design pressure ratio was good (0.91), a peak efficiency of 0.925 was obtained at a pressure ratio of 1.43 and at a specific weight flow of 34.0 pounds per second per square foot. At design speed the maximum pressure ratio obtained was 1.44. Peak efficiencies at 60, 80, and 115 percent design speed were 0.91, 0.94, and 0.87, respectively.

At all speeds the compressor system choked downstream of the outlet measuring station and therefore limited the minimum pressure ratio obtainable at maximum flow. Although the downstream area limited the flow through the compressor, it is apparent from the pressure-ratio curves of figure 4 that choking occurred within the rotor at design and 115 percent design speed and that a further reduction in the outlet pressure would not have substantially increased the weight flow even if the restriction in the compressor-outlet system were removed.

In comparison with the tapered-tip rotor configuration, the reset rotor increased the maximum pressure ratio and decreased the peak efficiency at all speeds. At design speed the reset rotor increased the maximum pressure ratio from 1.40 to 1.44 and decreased the peak efficiency from 0.95 to 0.925. The reset rotor also increased the maximum weight-flow capacity at all speeds. At design speed the reset rotor increased the maximum weight flow from 33.6 to 35.7 pounds per second per square foot frontal area.

The over-all performance of the reset tapered-tip 0.4 hub-tip diameter ratio rotor at design speed is compared with the over-all performance of the original rotor before any modifications were made in figure 5. The combination of tapering the tip and resetting the blades of the original 0.4 hub-tip diameter ratio rotor resulted in (1) increasing the maximum pressure ratio from 1.42 to 1.44, (2) increasing the maximum specific weight flow from 34.1 to 35.7 pounds per second per square foot of frontal area, and (3) approximately doubling the weight-flow range. As shown by figure 5, the peak efficiency of the rotor at design speed was unchanged by the rotor modifications.

Rotor Flow Parameters

Rotor inlet flow parameters. - The radial variation of the inlet axial Mach number, the relative inlet Mach number, and the relative inlet air angle are presented in figure 6 for the near-maximum, near-average, and near-minimum weight-flow conditions at design speed. Included in figure 6 are the respective design values of each parameter. The distribution of the inlet axial Mach number for the reset tapered-tip rotor was taken the same as the distribution of the inlet axial Mach number of reference 4. The actual distribution of the inlet axial Mach number for the reset tapered-tip rotor (fig. 6) agreed with that of reference 4, but the magnitude of the Mach number was less because of the lower-than-design value of weight flow obtained. The major difference between the design and actual values of inlet axial Mach number, relative inlet Mach number, and the relative inlet air angle can therefore be attributed to the lower-than-design values of weight flow obtained.

Rotor outlet flow parameters. - The radial variations of efficiency, relative total-pressure-loss coefficient, dimensionless work coefficient, total-pressure ratio, absolute and relative outlet Mach numbers, absolute outlet air angle, and relative outlet air angle are presented in figure 7 for the near-maximum, near-average, and near-minimum weight-flow conditions at design speed.

The rotor efficiency, in general, decreased steadily from the rotor hub to the rotor tip. At the near-maximum weight flow (35.17) the efficiency decreased from a peak value of 0.95 approximately 30 percent from the hub to 0.86 at 10 percent of the passage height from the outer wall. The relative total-pressure-loss coefficient reached a minimum value approximately 30 percent of the passage height from the inner wall and increased sharply toward the outer wall. At the near-maximum weight flow the energy addition increased from the hub section to a maximum value at the mean passage section and then decreased toward the tip section. However, as the weight flow was decreased, the energy addition tended to increase steadily from the hub to the tip section. The total-pressure ratio, in general, increased from the rotor hub to the mean radius and then decreased sharply toward the rotor tip.

At the near-maximum weight flow the absolute outlet Mach number varied from approximately 0.94 at the hub section to 0.78 at the tip section. The relative outlet Mach number, in general, increased directly with radius and at the near-maximum weight flow increased from 0.73 at the hub section to a maximum value of 0.88 at the tip section.

For the near-maximum weight flow, the absolute outlet air angle varied from approximately 39° at the hub section to 24° at the tip section. The relative outlet air angle increased with increased radius. At all weight flows the relative outlet air angles were approximately 5°

past the axial direction at 10 percent of the passage height from the inner wall. This is approximately the same degree of turning past the axial direction that was obtained with the transonic rotor of reference 6.

The radial variation of the axial velocity after the rotor is presented in figure 8 for the near-peak-efficiency weight flow at design speed as a ratio of the axial velocity to the mean-radius axial velocity. Included in figure 8 is the axial-velocity distribution predicted by simple radial equilibrium equation with entropy gradients (ref. 9) as applied to the measured outlet conditions. The difference between the actual velocity distribution and that predicted by the radial equilibrium solution is small and can probably be attributed to the effect of streamline curvature, which was neglected in the solution.

Blade-element flow parameters. - The blade-element flow parameters (total-pressure-loss coefficient, relative inlet Mach number, efficiency, axial-velocity ratio, diffusion factor, static-pressure-rise coefficient, deviation angle, dimensionless work coefficient, and total-pressure ratio) are presented in figure 9 to supplement the published data on transonic rotor-blade performance. The data are presented as a function of incidence angle for the five major radial stations (10, 30, 50, 70, and 90 percent of the passage height from the outer wall).

Radial matching of blade-element sections. - The radial variation of incidence angle for the various weight flows at design speed is presented in figure 10. Included in figure 10 are the design values of the minimum-loss incidence angle and the minimum-loss incidence angles obtained from the blade-element data of figure 9 for each of the five blade-element sections. As shown by figure 10, the incidence-angle variation at a weight flow of 35.17 pounds per second per square foot was within 1° of the minimum-loss incidence angle at all blade sections. The minimum-loss incidence angles, however, varied from approximately 0.8° higher than the design value at the tip section to 2.5° higher than the design value at the hub section. This increase in the minimum-loss incidence angle above the design value caused the weight flow to be lower than the design value.

COMPARISON OF BLADE-ELEMENT PERFORMANCE AND DESIGN RULES

A comparison of the blade-element performance and design rules of reference 8 is tabulated in table I for the five major radial stations at design speed. The blade-element performance parameters (incidence angle, deviation angle, and total-pressure-loss coefficient) were obtained from figure 9 for each blade-element section at the minimum-loss incidence angle. The corresponding values of relative inlet Mach number, relative inlet air angle, relative outlet air angle, blade thickness, and

solidity were then used in conjunction with the design rules of reference 8 to determine the design values of minimum-loss incidence angle, deviation angle, and total-pressure-loss coefficient.

As shown by table I, the minimum-loss incidence angle was 0.9° to 2.8° greater than the values predicted by the design rule except at the hub section, where the minimum-loss incidence angle was 6.2° greater than the value predicted by the design rule. The deviation angle at the minimum-loss incidence angle (table I) was 1.6° to 3° less than the values predicted by the design rule at the 10, 30, 50, and 70 percent passage sections. At the hub section the deviation angle was 4.5° greater than the value predicted by the design rule. The total-pressure-loss parameter is presented in table I as $\omega \cos \beta_2'/2\sigma$ so as to be consistent with that in reference 8. As shown by table I, the total-pressure-loss parameter is considerably greater than the values predicted by the design rule over the complete passage. Although the agreement between the data and the design-rule predictions is not considered good, the minimum-loss incidence angles were matched radially (fig. 10) so that high compressor efficiency was obtained but at a weight flow below the design value.

4207

CZ-2

MINIMUM-LOSS AND CHOKING INCIDENCE-ANGLE ANALYSIS AT ROTOR HUB SECTION

As pointed out previously, the $4\frac{1}{2}^\circ$ increase in the minimum-loss incidence angle at the hub section resulting from resetting the blades was not anticipated from the design incidence-angle rules of reference 8. The design incidence-angle rule of reference 8 was determined from the performance of 17 different transonic rotors, one of which was the original 0.4 hub-tip diameter ratio rotor (ref. 7).

For comparison purposes the incidence-angle rule of reference 8, which gives the variation of the difference between the minimum-loss rotor incidence angle and the cascade-rule incidence angle with relative inlet Mach number, is presented in figure 11. Included in figure 11 are data from reference 10. The data points in figure 11 which represent the original 0.4 hub-tip diameter ratio rotor (before tip was tapered) are marked and fall on the upper limits of the data for the rotors investigated.

The data points for the reset tapered-tip 0.4 hub-tip diameter ratio rotor are included in figure 11 and fall above the limits established by the other transonic rotors. It therefore appears that the present rotor choked before the other reference rotors and increased the minimum-loss incidence angle because of its low blade setting angle of 6.6° or because of the nature of its inherent three-dimensional flow.

In cases where rotors are designed for blade and passage geometry which deviate from the geometry of the rotors of reference 8, it appears

[redacted]

that a more complete analysis for determining blade choking should be employed. One such complete analysis on blade choking is reference 11, in which the effect of streamline curvature and contraction in the meridian plane as well as the complete flow from blade to blade is considered. Although the complete solution of reference 11 is recommended, it is lengthy and time consuming and may in some cases be replaced by the simplified empirical blade-choking analysis of reference 12.

In reference 12 the difference between the minimum-loss incidence angle and an empirical choking incidence angle is presented as a function of relative inlet Mach number for double-circular-arc blades. The empirical incidence angle used in reference 12 is the incidence angle at which the upstream stream-tube area is equal to the blade throat area. The correlation obtained for the rotor hub section in reference 12 is presented in figure 12 together with additional data of reference 6. Included in figure 12 are the data points of the original 0.4 hub-tip diameter ratio rotor (before tip was tapered) and the data points of the reset tapered-tip 0.4 hub-tip diameter ratio rotor. The data points for both of the 0.4 hub-tip diameter ratio rotors fall within the variation of the other transonic rotors. Figure 12 also includes the data of reference 6, in which the design relative outlet air was also turned approximately 5° past the axial direction but with a somewhat greater value of relative inlet Mach number. It therefore appears that the minimum-loss incidence-angle analysis of reference 12 is applicable over a wide range of rotor geometry configurations including the case of low blade-setting angles where the relative outlet air is turned up to 5° past the axial direction.

In line with the throat-area choking analysis of reference 12, the experimental throat area for the 0.4 hub-tip diameter ratio rotor before resetting the blades was calculated. Equation (1) of reference 12 was rearranged to give:

$$\frac{d}{s} = \cos(\beta_b + i_{ch})\left(\frac{A_{cr}}{A}\right)_{M_1'}$$

By using the experimental data of reference 4 for the choke point at design speed, all terms in equation (1) were known except the ratio of the throat area per unit spacing (throat height is normalized through division by blade spacing). Therefore, from the experimental data ($i_{ch} = 6.6°$, $M_1' = 0.65$, and $\beta_b = 32.8$) an effective throat area d/s of 0.681 was calculated for the 0.4 hub-tip diameter ratio tapered-tip rotor at design speed. At 105 and 115 percent design speed, the effective throat areas were calculated to be 0.684 and 0.695, respectively. Therefore, it appears that rotor choking at design, at 105 percent design, and at 115 percent design speed occurred at approximately the same effective throat area.

In resetting the blades of the 0.4 hub-tip diameter-ratio tapered-tip rotor, an enlarged conical-plane layout of the blade sections at the hub (10 percent from the inner wall) showed that the two-dimensional throat area increased 6.5 percent. It was then assumed that at design speed experimental throat areas of the reset blades would also increase 6.5 percent. From equation (1) with the new value of $d/s = 1.065 \times 0.681$ known, the choking incidence angle and inlet Mach number for the reset blade were calculated to be 10.3° and 0.67, respectively. Since the actual choking incidence angle for the reset blade at the hub was 10.8° at a Mach number of 0.69, it appears that the ratio of the actual and effective areas was the same for both rotor configurations. In applying the same analysis for the 115-percent-design-speed case for the reset blade, the calculated choking incidence angle and Mach number were found to be 13.8° and 0.74, respectively, as compared with the actual choking incidence angle of 13.5° and Mach number of 0.75.

This later experimental choking-incidence-angle analysis only served to indicate that, when rotor geometry varies appreciably from the rotor geometry on which minimum-loss empirical incidence-angle rules are based, choking incidence angle should be investigated to ensure that the selected minimum-loss incidence angle is greater than the choking incidence angle for the given rotor configuration.

SUMMARY OF RESULTS

The blades of the tapered-tip 0.4 hub-tip diameter ratio rotor were reset $7\frac{1}{2}^\circ$ in the rotor disk and twisted linearly from 0° at the mean-radius section to $4\frac{1}{2}^\circ$ at the tip section to increase the specific weight flow approximately 10 percent to 36.3 pounds per second per square foot of frontal area. The performance of the reset rotor was analyzed and the following results were obtained:

1. At design speed the reset tapered-tip rotor produced the design pressure ratio of 1.38 at a specific weight flow at 35.6 pounds per second per square foot at an efficiency of 0.91. A peak efficiency of 0.925 was obtained at a specific weight flow of 34.0 pounds per second per square foot. A maximum pressure ratio of 1.44 and a maximum weight flow of 35.7 pounds per second per square foot were obtained. Peak efficiencies at 60, 80, and 115 percent design speed were 0.91, 0.94, and 0.87, respectively.

2. In comparison with the tapered-tip rotor, the reset tapered-tip rotor at design speed increased the maximum pressure ratio from 1.40 to 1.44 and decreased the peak efficiency from 0.95 to 0.925. The reset rotor also increased the maximum specific weight flow from 33.6 to 35.7 pounds per second per square foot of frontal area.

[redacted]

3. The radial selection of the blade-element parameters was sufficiently good so that high compressor efficiency was obtained but at a weight flow below the design value.

4. At the rotor hub section where the relative outlet air was turned 5° past the axial direction, the design-speed minimum-loss incidence angle was on the upper limit of the values predicted by one of the previously published design rules and over the limits of another. The analysis pointed out that, when a rotor geometry deviates from the rotor geometry used to derive an empirical minimum-loss incidence-angle rule, an independent analysis should be made to determine that the selected minimum-loss incidence angle is greater than the choking incidence angle for the given rotor configuration.

Lewis Flight Propulsion Laboratory
National Advisory Committee for Aeronautics
Cleveland, Ohio, December 6, 1956

APPENDIX - SYMBOLS

(A_{cr}/A)	ratio of critical area (sonic flow) to actual flow area at any point of flow
A_f	compressor frontal area, sq ft
c	blade chord, in.
D	diffusion factor
d	distance between blades at rotor throat, in.
H	total enthalpy, ft-lb/lb
i	angle of incidence, angle between tangent to blade mean camber line at leading edge and inlet-air direction, deg
M	Mach number
P	total pressure, lb/sq ft
p	static pressure, lb/sq ft
r	radius, in.
s	blade spacing, in.
T	total temperature, ^{o}R
t	blade thickness, in.
U	blade speed, ft/sec
V	velocity of air, ft/sec
W	integrated weight flow at rotor inlet, lb/sec
β	angle between velocity vector and rotor axis, deg
β_b	blade inlet angle, angle between tangent to blade mean camber line and rotor axis at blade leading edge, deg
γ^{o}	blade setting angle, angle between blade chord and rotor axis, deg
δ	ratio of inlet total pressure to standard NACA sea-level pressure, P/2116.2

[redacted]

δ^o	deviation angle, angle between tangent to mean camber line at blade trailing edge and axis direction, deg
η	adiabatic efficiency
θ	ratio of inlet total temperature to standard NACA sea-level temperature, T/518.6
ρ	static air density, slugs/cu ft
σ	solidity ratio, ratio of blade chord to blade spacing
φ	blade camber angle, deg
ω	total-pressure-loss coefficient

Subscripts:

ch	choke
d	design rule
m	mean radius
min	minimum loss
t	rotor tip
z	axial direction
θ	tangential direction
1	rotor inlet
2	rotor outlet
2-D	two-dimensional

Superscript:

'	relative

REFERENCES

1. Robbins, William H., and Glaser, Frederick W.: Investigation of an Axial-Flow-Compressor Rotor with Circular-Arc Blades Operating up to a Rotor-Inlet Relative Mach Number of 1.22. NACA RM E53D24, 1953.

2. Lieblein, Seymour, Lewis, George W., Jr., and Sandercock, Donald M.: Experimental Investigation of an Axial-Flow Compressor Inlet Stage Operating at Transonic Relative Inlet Mach Numbers. II - Over-All Performance of Stage with Transonic Rotor and Subsonic Stators up to Rotor Relative Inlet Mach Number of 1.1. NACA RM E52A24, 1952.

3. Serovy, George K., Robbins, William H., and Glaser, Frederick W.: Experimental Investigation of a 0.4 Hub-Tip Diameter Ratio Axial-Flow Compressor Inlet Stage at Transonic Inlet Relative Mach Numbers. I - Rotor Design and Over-All Performance at Tip Speeds from 60 to 100 Percent of Design. NACA RM E53I11, 1953.

4. Montgomery, John C., and Glaser, Frederick W.: Experimental Investigation of a 0.4 Hub-Tip Diameter Ratio Axial-Flow Compressor Inlet Stage at Transonic Inlet Relative Mach Numbers. III - Effect of Tip Taper on Over-All and Blade Element Performances. NACA RM E55L09, 1956.

5. Schwenk, Francis C., Lewis, George W., Jr., and Lieblein, Seymour: Experimental Investigation of an Axial-Flow-Compressor Inlet Stage Operating at Transonic Relative Inlet Mach Numbers. V - Rotor Blade-Element Performance at a Reduced Blade Angle. NACA RM E56J17, 1956.

6. Wright, Linwood C., and Wilcox, Ward W.: Investigation of Two-Stage Counterrotating Compressor. II - First-Rotor Blade-Element Performance. NACA RM E56G09, 1956.

7. Montgomery, John C., and Glaser, Frederick W.: Experimental Investigation of a 0.4 Hub-Tip Diameter Ratio Axial-Flow Compressor Inlet Stage at Transonic Inlet Relative Mach Numbers. II - Stage and Blade-Element Performance. NACA RM E54I29, 1955.

8. Robbins, William H., Jackson, Robert J., and Lieblein, Seymour: Blade-Element Flow in Annular Cascades. Ch. VII of Aerodynamic Design of Axial-Flow Compressors, vol. II. NACA RM E56B03a, 1956.

9. Hatch, James E., Giamati, Charles C., and Jackson, Robert L.: Application of Radial-Equilibrium Condition to Axial-Flow Turbomachine Design Including Consideration of Change of Entropy with Radius Downstream of Blade Row. NACA RM E54A20, 1954.

[redacted]

10. Creagh, John W. R.: Performance Characteristics of an Axial-Flow Transonic Compressor Operating up to Tip Relative Inlet Mach Number of 1.34. NACA RM E56D27, 1956.

11. Stewart, Warner L.: Analytical Investigation of Flow Through High-Speed Mixed-Flow Turbine. NACA RM E51H06, 1951.

12. Wright, Linwood C., and Schwind, Richard: Throat-Area Determination for a Cascade of Double-Circular-Arc Blades. NACA RM E55H25a, 1955.

TABLE I. - COMPARISON OF BLADE-ELEMENT PERFORMANCE AND DESIGN RULES[a]

Passage height from tip, percent	Blade camber angle, φ, deg	Blade thickness ratio, t/c	Solidity ratio, σ	Relative inlet angle, β_1, deg	Relative inlet Mach number, M_1'	Incidence angle, deg			Deviation angle, deg			Total-pressure-loss coefficient	
						i_{min}	i_d	$i_{min}-i_d$	δ	δ_d	$\delta-\delta_d$	$\frac{\omega \cos \beta_2'}{2\sigma}$	$\left(\frac{\omega \cos \beta_2'}{2\sigma}\right)_d$
10	14.6	0.053	0.98	53.8	1.08	4.8	3.0	1.8	1.7	3.9	-2.2	0.027	0.011
30	19.1	.059	1.10	49.1	1.00	5.6	4.7	.9	2.2	5.2	-3.0	.031	.008
50	24.7	.065	1.27	45.7	.90	8.4	5.6	2.8	3.5	6.5	-3.0	.019	.008
70	30.8	.071	1.48	40.8	.80	9.0	6.2	2.8	5.5	7.1	-1.6	.017	.005
90	37.7	.077	1.79	37.3	.67	12.0	5.8	6.2	12.4	7.9	4.5	.018	.005

[a]Ref. 8.

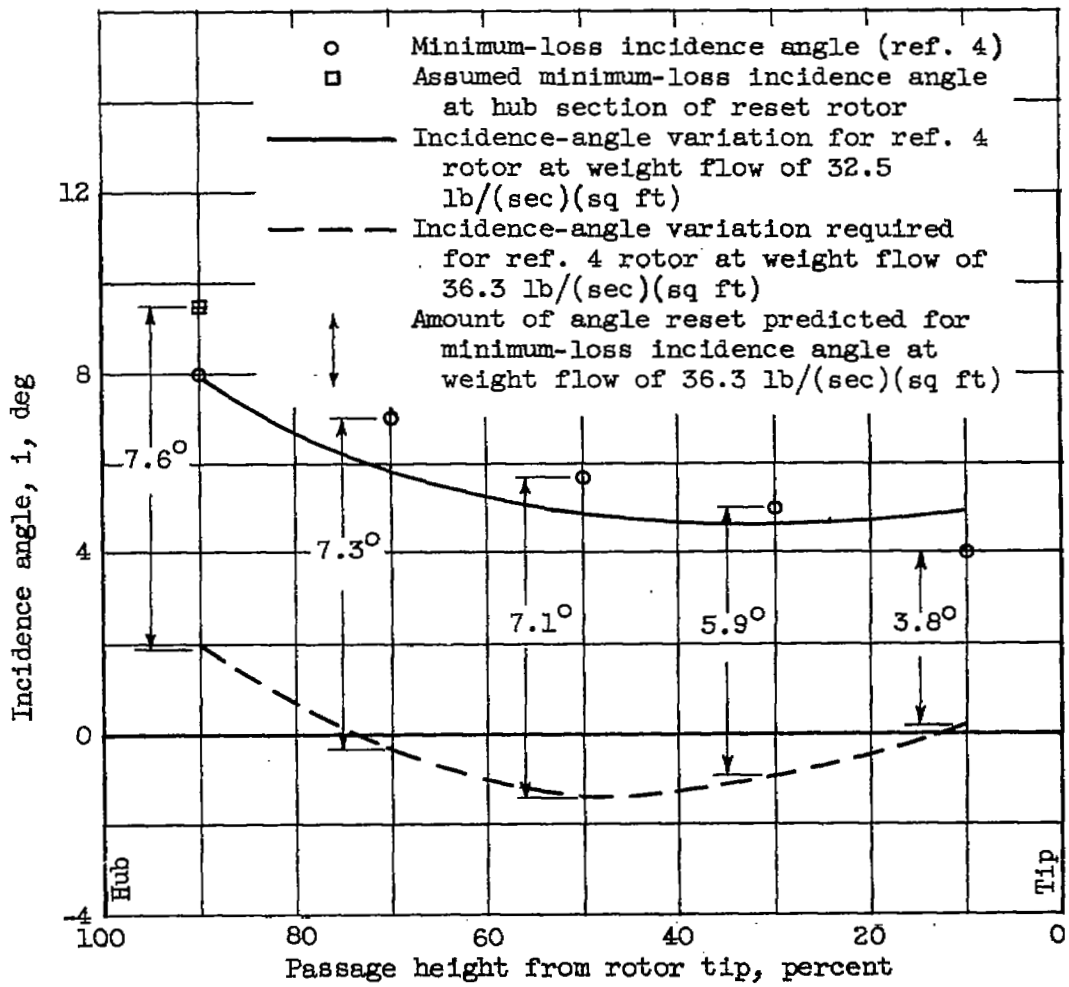

Figure 1. - Incidence-angle variation for tapered-tip 0.4 hub-tip diameter ratio rotor of reference 4 at design speed.

[redacted]

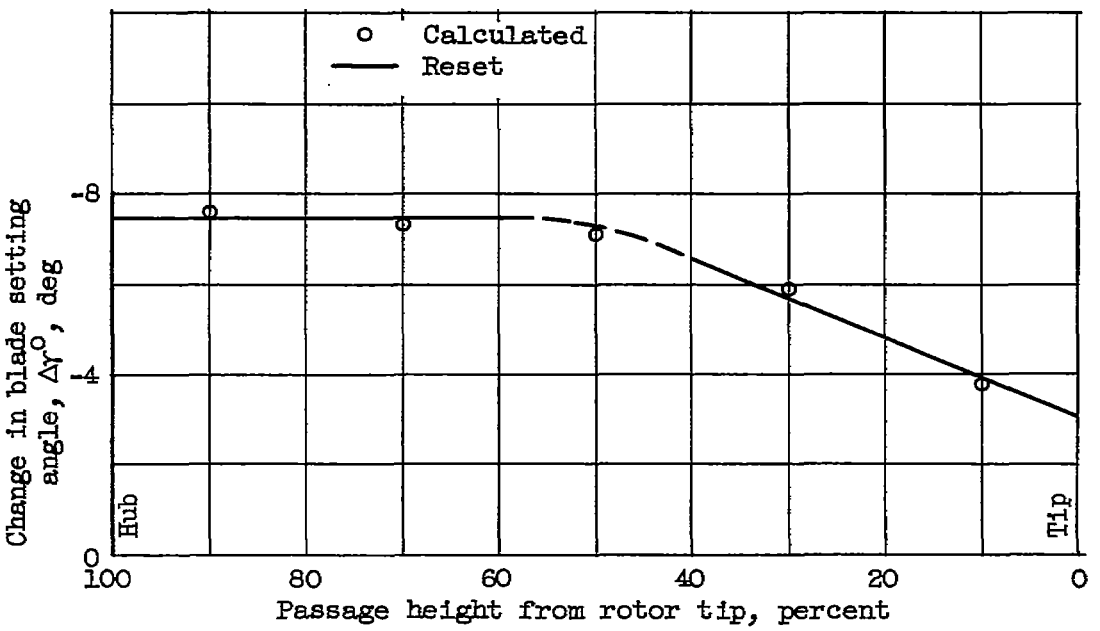

Figure 2. - Calculated and actual change of blade setting angle required for increasing weight flow approximately 10 percent (36.3 lb/(sec)(sq ft)) at design speed.

[redacted]

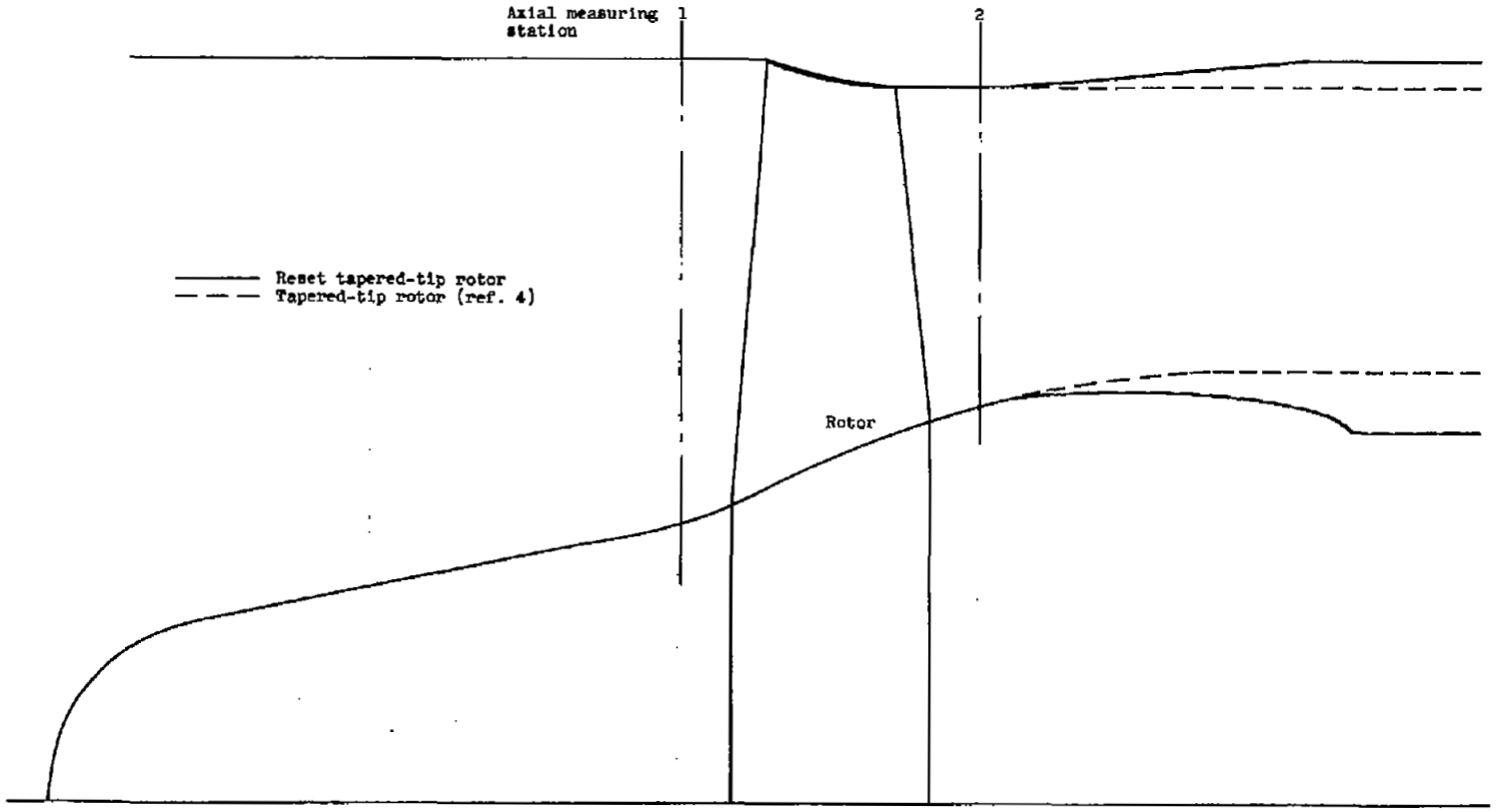

Figure 3. - Outlet-passage modification for tapered-tip 0.4 hub-tip diameter ratio transonic rotor with reset blade angles.

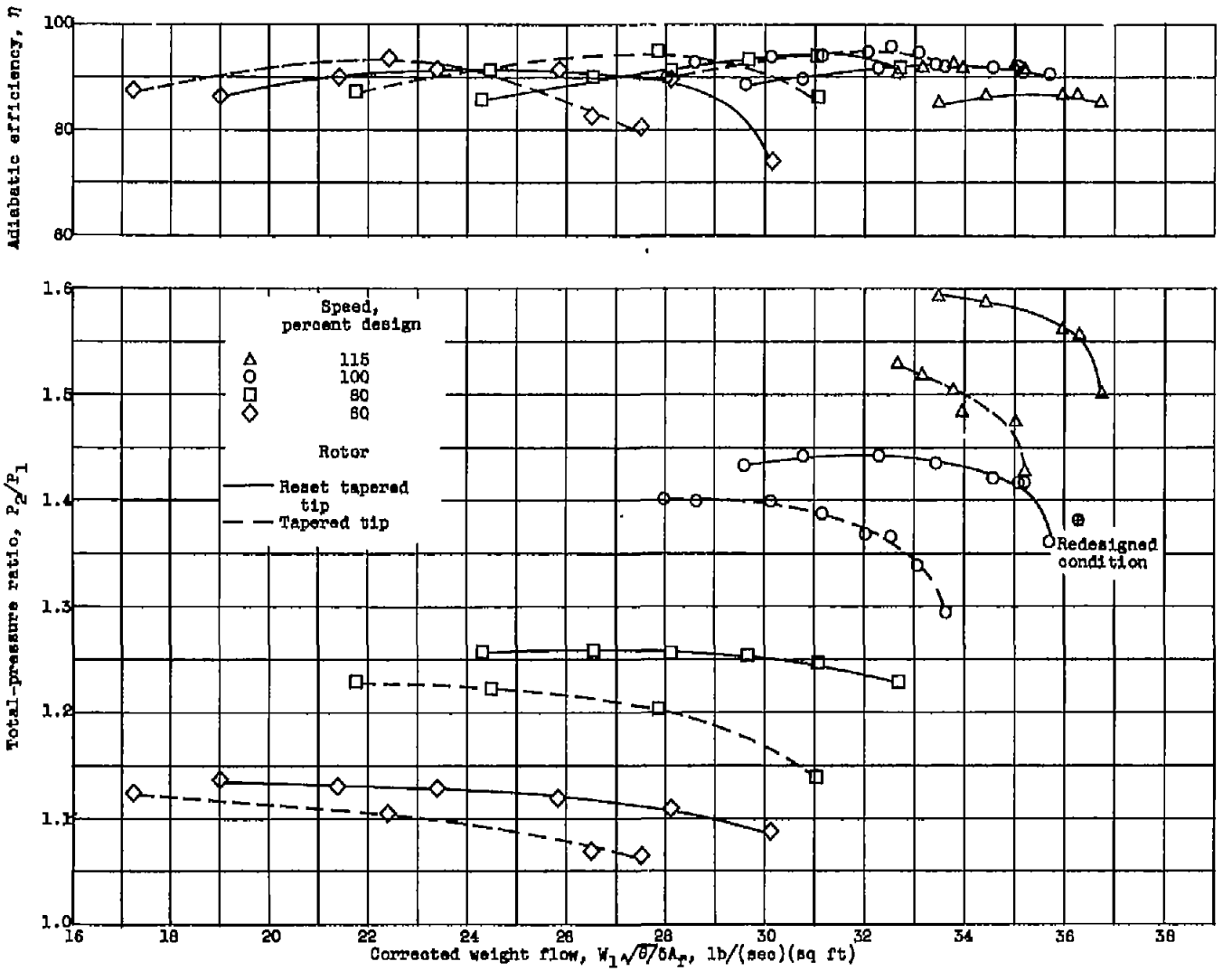

Figure 4. - Over-all performance of 0.4 hub-tip diameter ratio tapered-tip rotor before and after resetting blades.

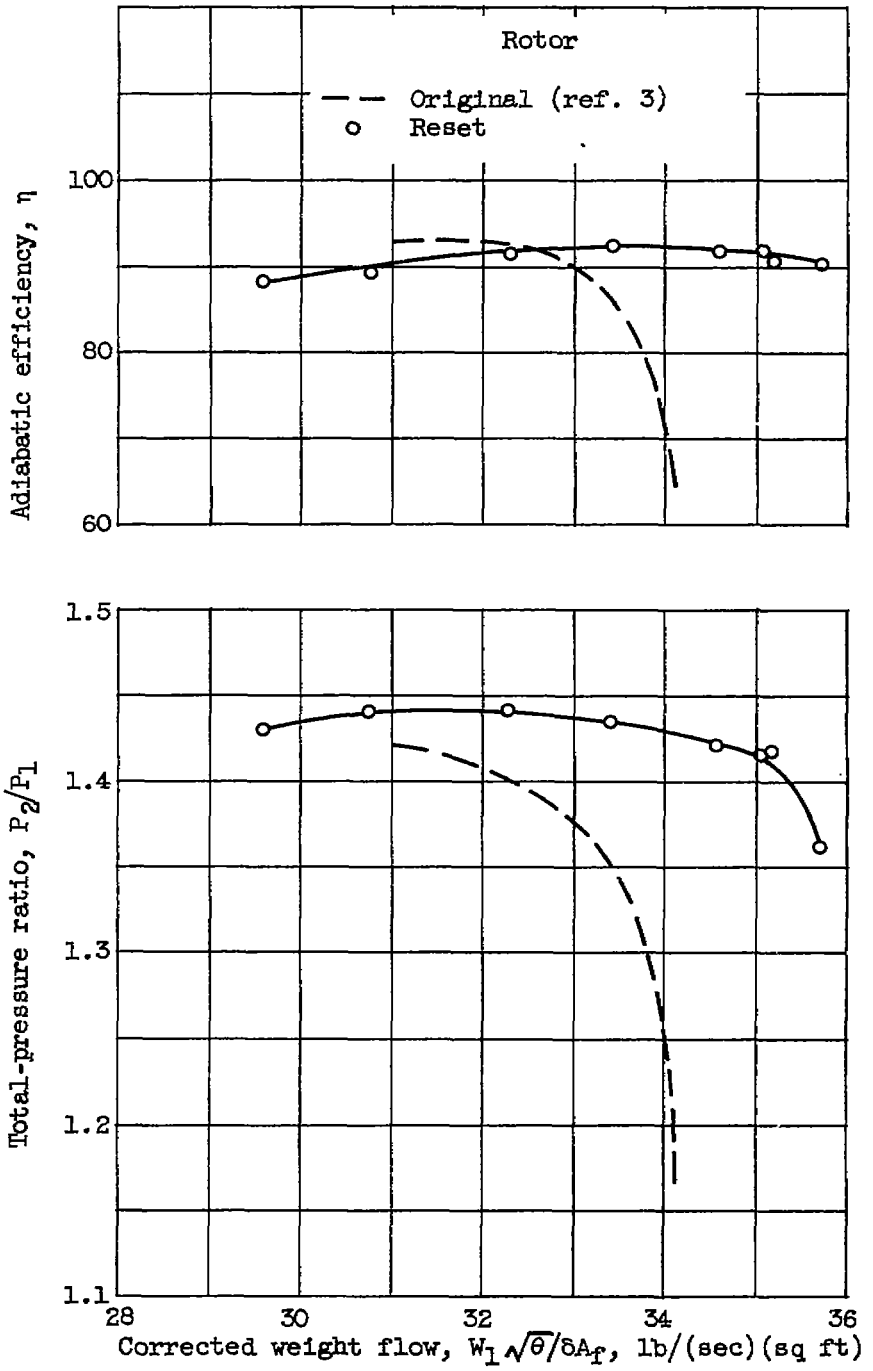

Figure 5. - Comparison of over-all performance of reset tapered-tip rotor with original 0.4 hub-tip diameter ratio rotor at design speed.

[redacted]

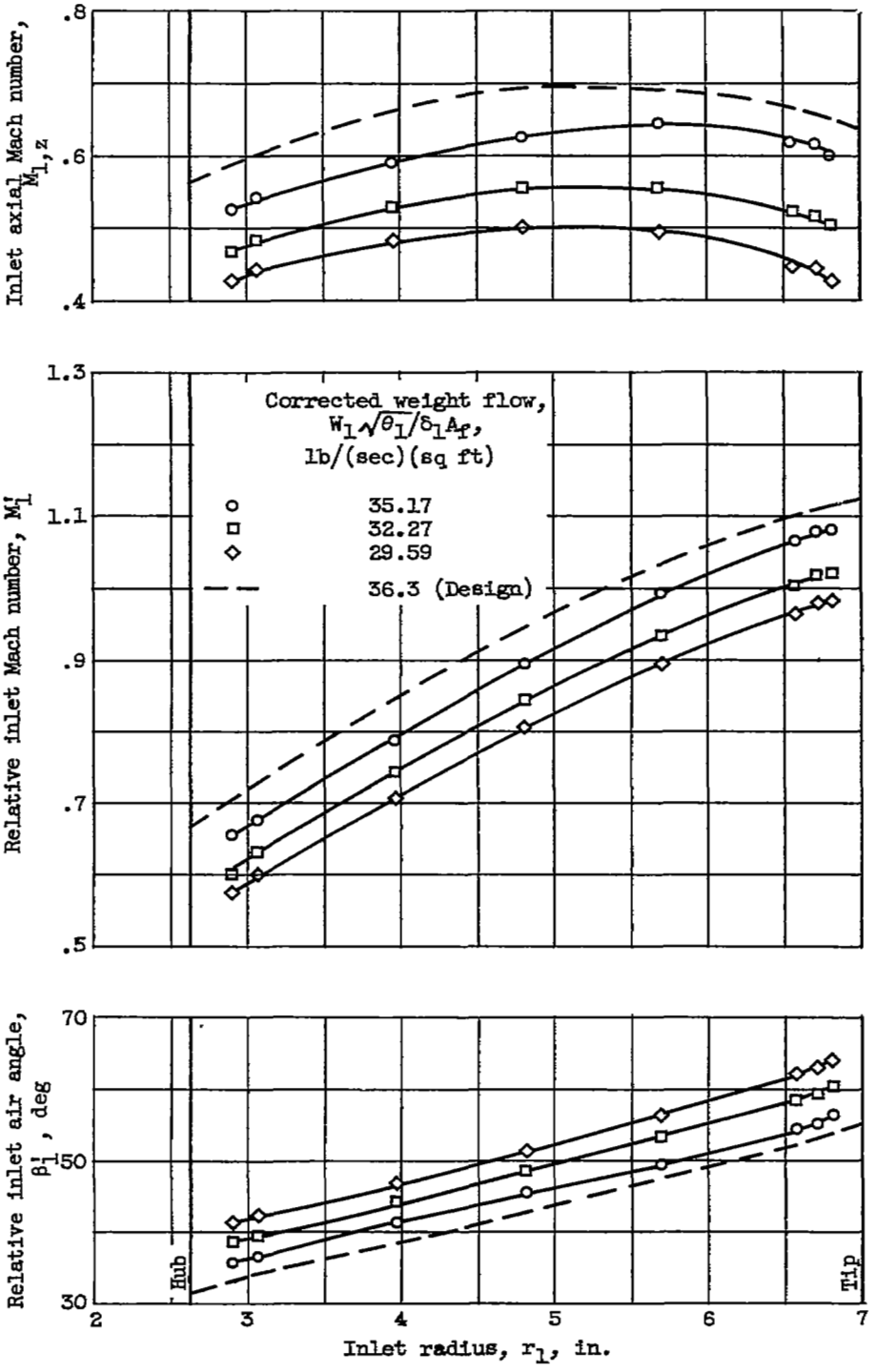

Figure 6. - Radial variation of rotor inlet flow parameters at design speed.

[redacted]

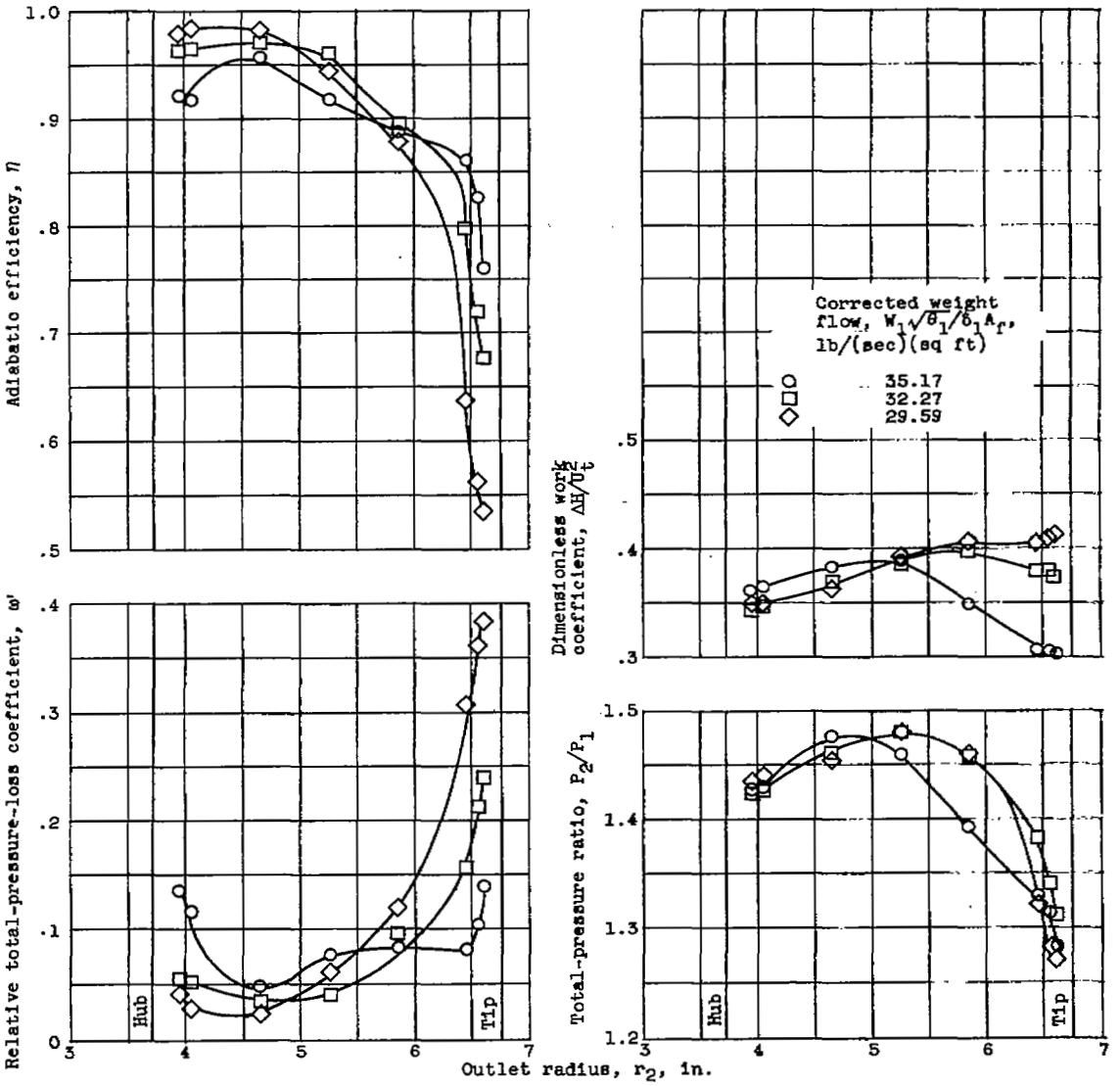

Figure 7. - Radial variation of rotor outlet flow parameters at design speed.

[redacted]

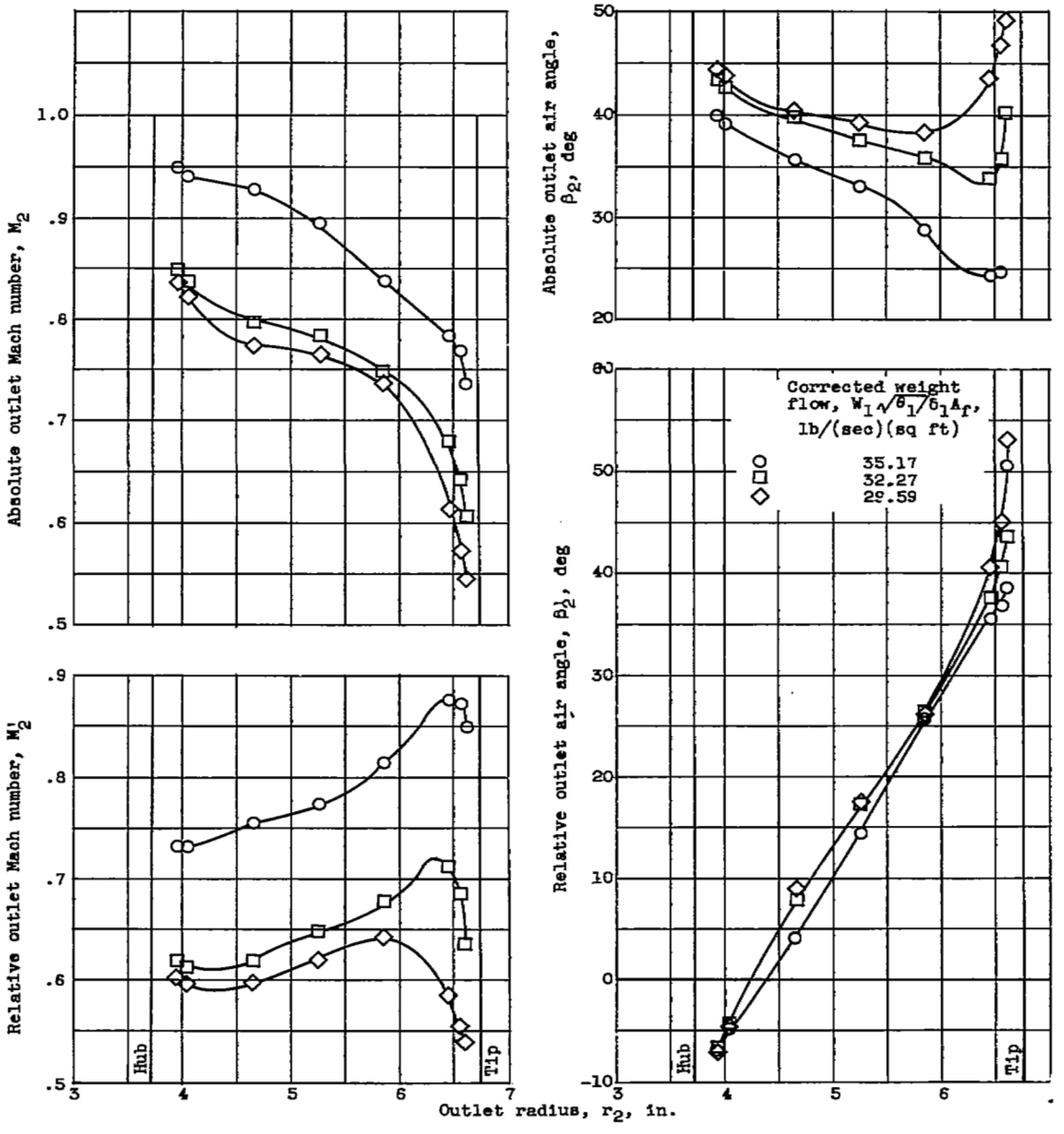

Figure 7. - Concluded. Radial variation of rotor outlet flow parameters at design speed.

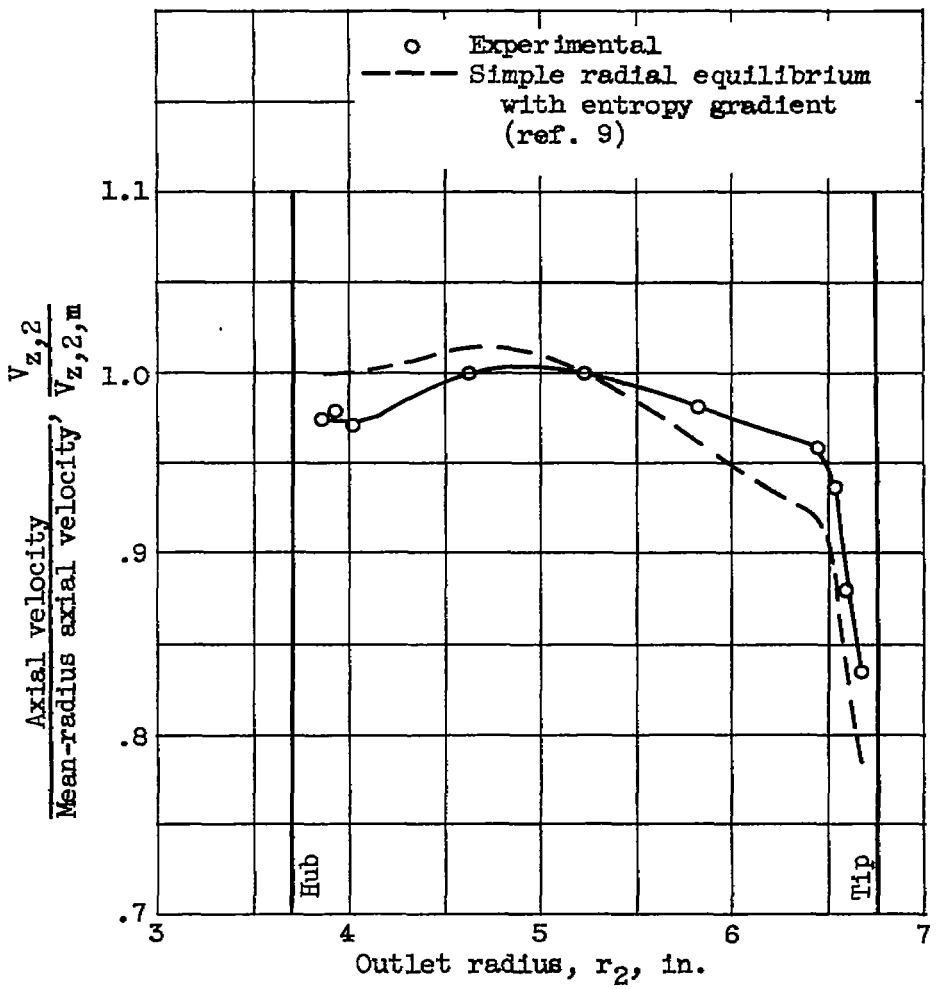

Figure 8. - Radial equilibrium comparison of rotor outlet axial velocity for near over-all peak-efficiency weight flow at design speed.

[redacted]

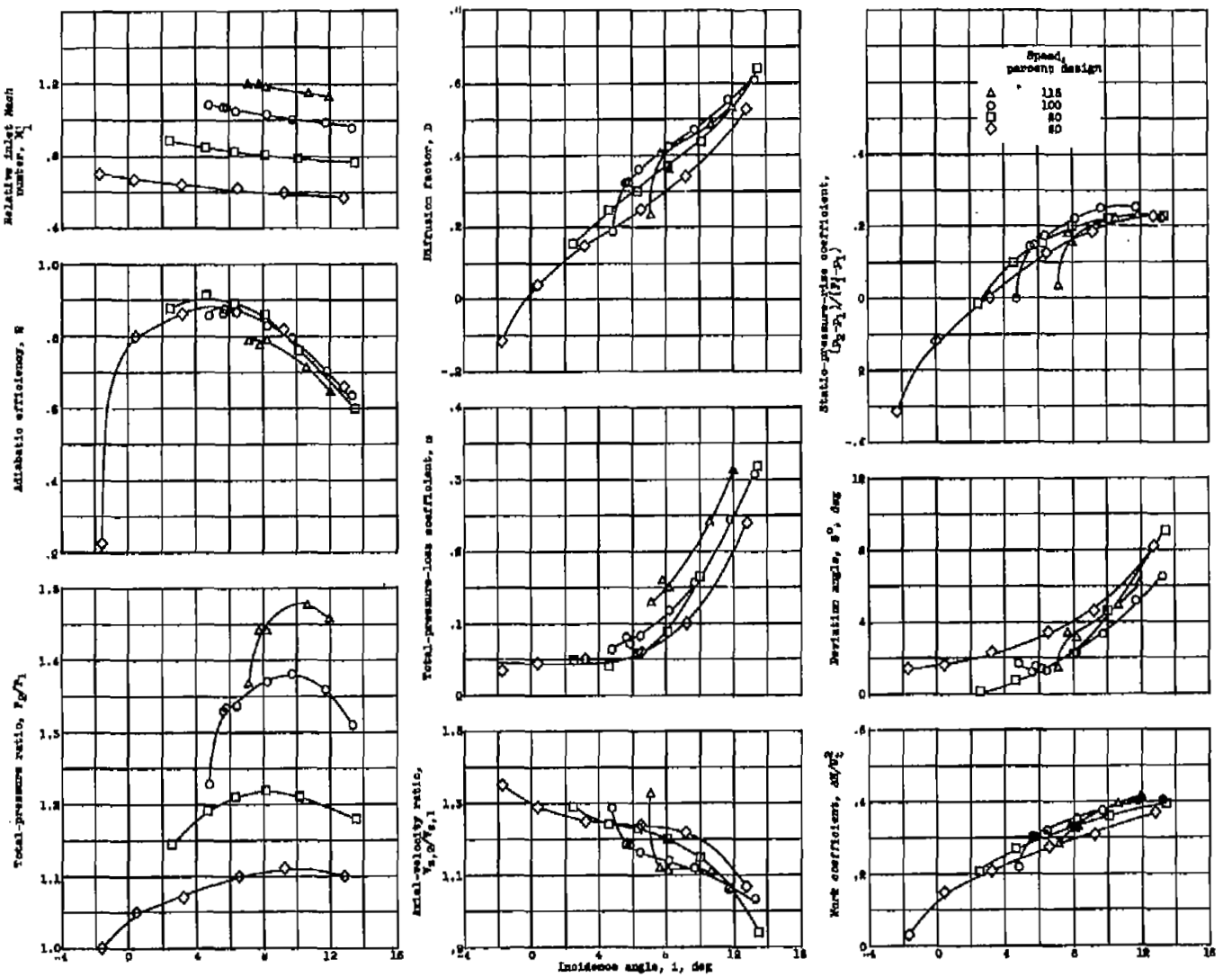

(a) 10 Percent of passage height from tip; inlet radius, 6.56 inches.

Figure 9. - Reset tapered-tip rotor-blade-element data.

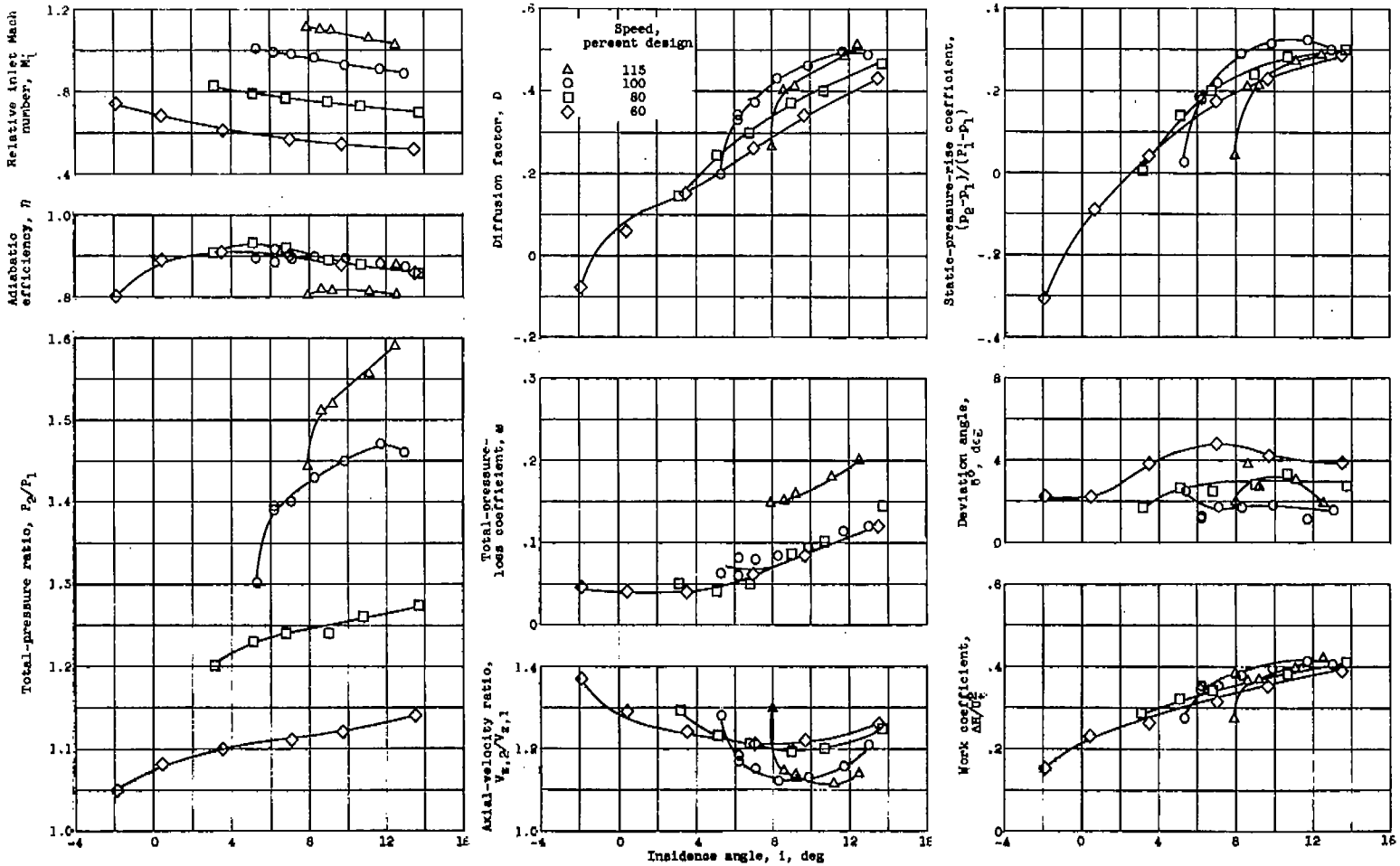

(b) 30 Percent of passage height from rotor tip; inlet radius, 5.69 inches.

Figure 9. - Continued. Reset tapered-tip rotor-blade-element data.

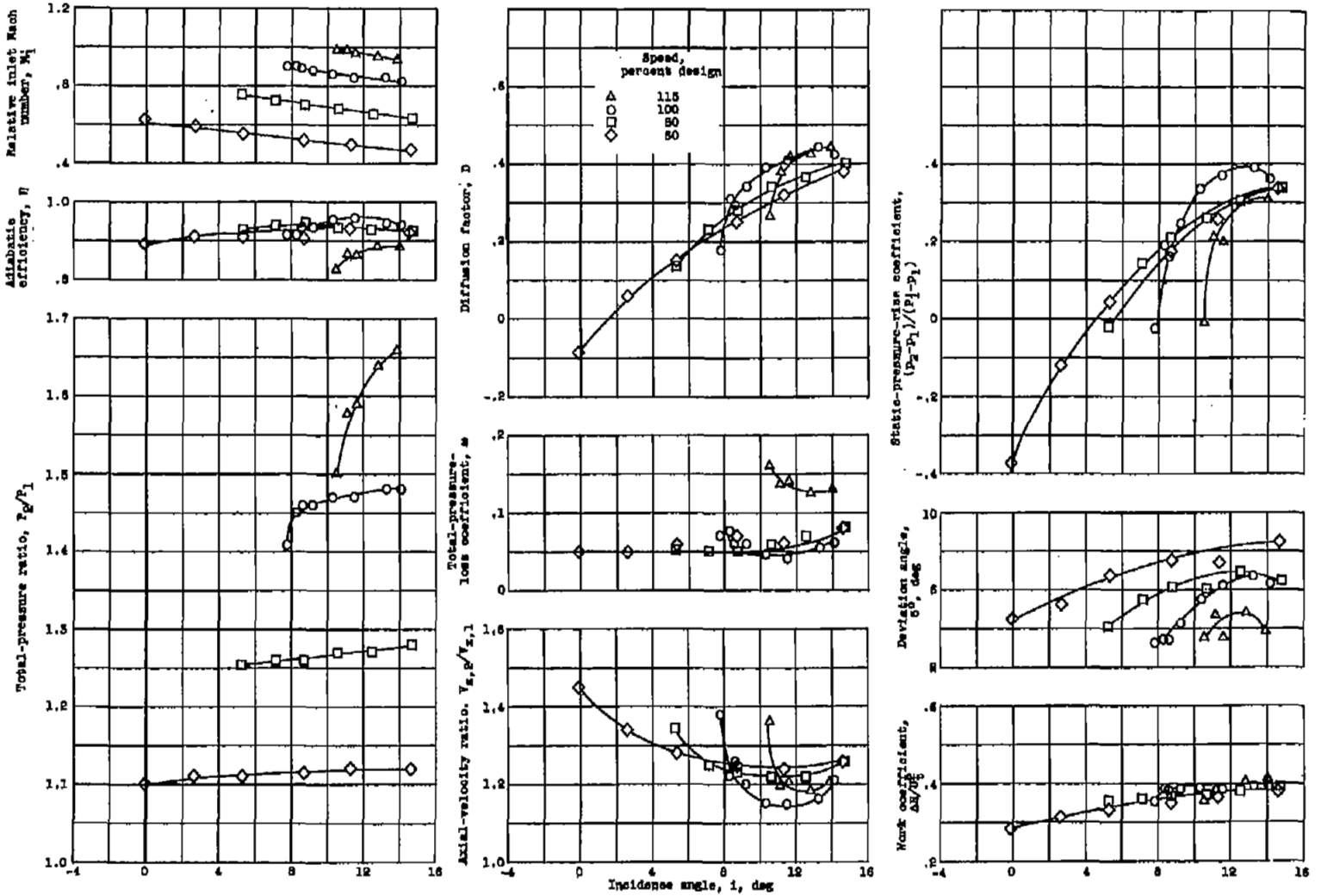

(c) 50 Percent of passage height from rotor tip; inlet radius, 4.82 inches.

Figure 9. - Continued. Reset tapered-tip rotor-blade-element data.

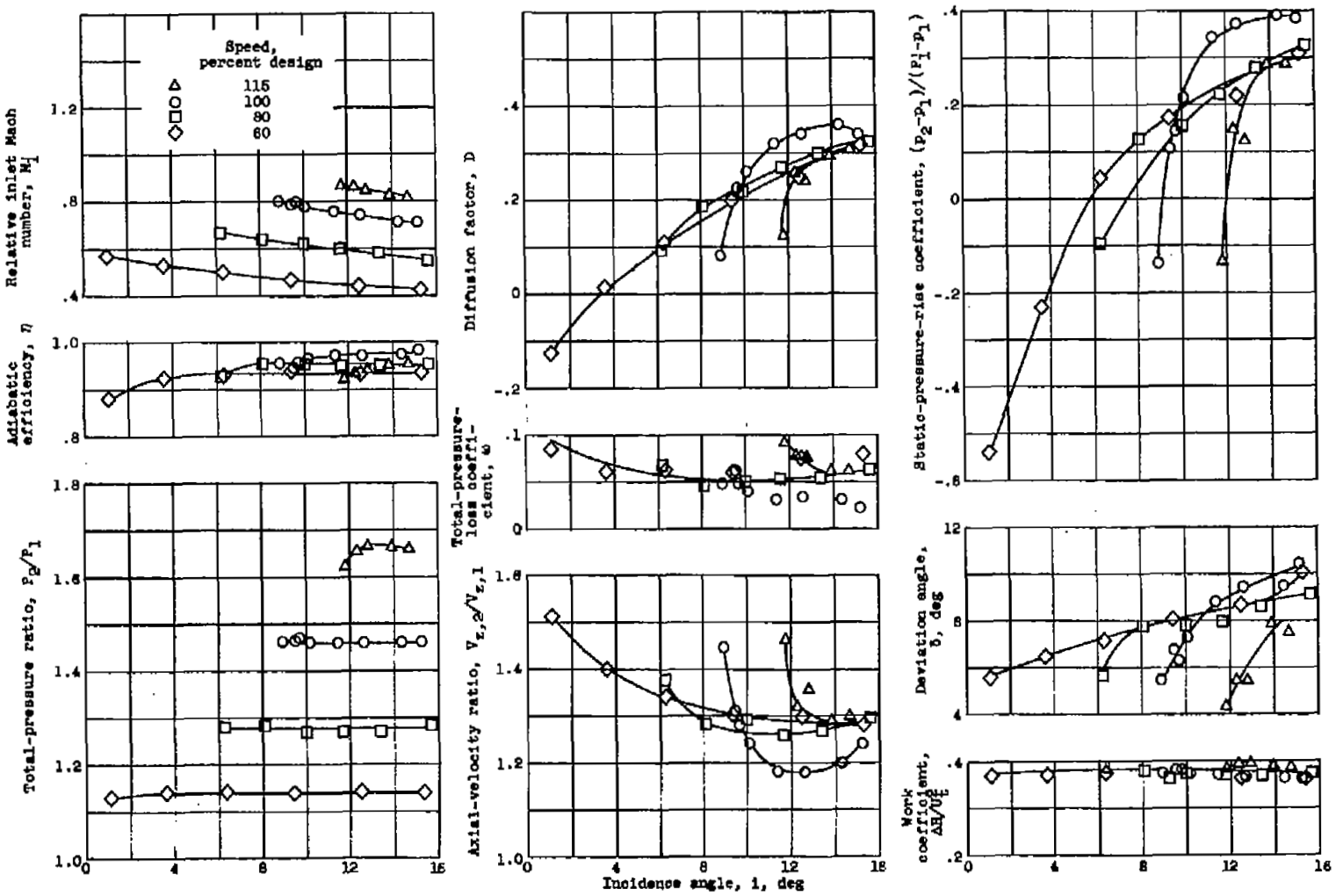

(d) 70 Percent of passage height from tip; inlet radius, 3.95 inches.

Figure 9. - Continued. Reset tapered-tip rotor-blade-element data.

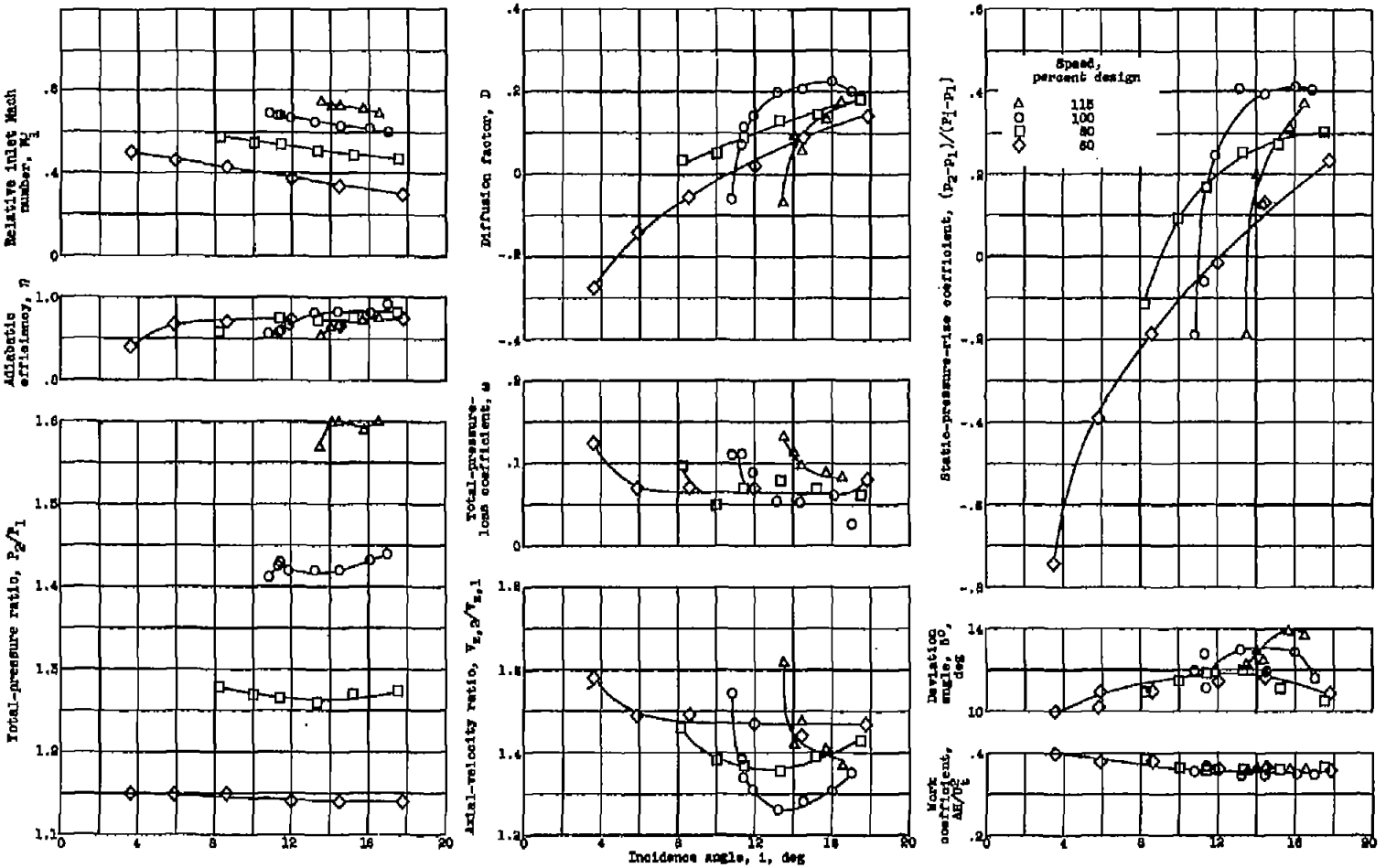

(e) 90 Percent of passage height from tip; inlet radius, 3.08 inches.

Figure 9. - Concluded. Reset tapered-tip rotor-blade-element data.

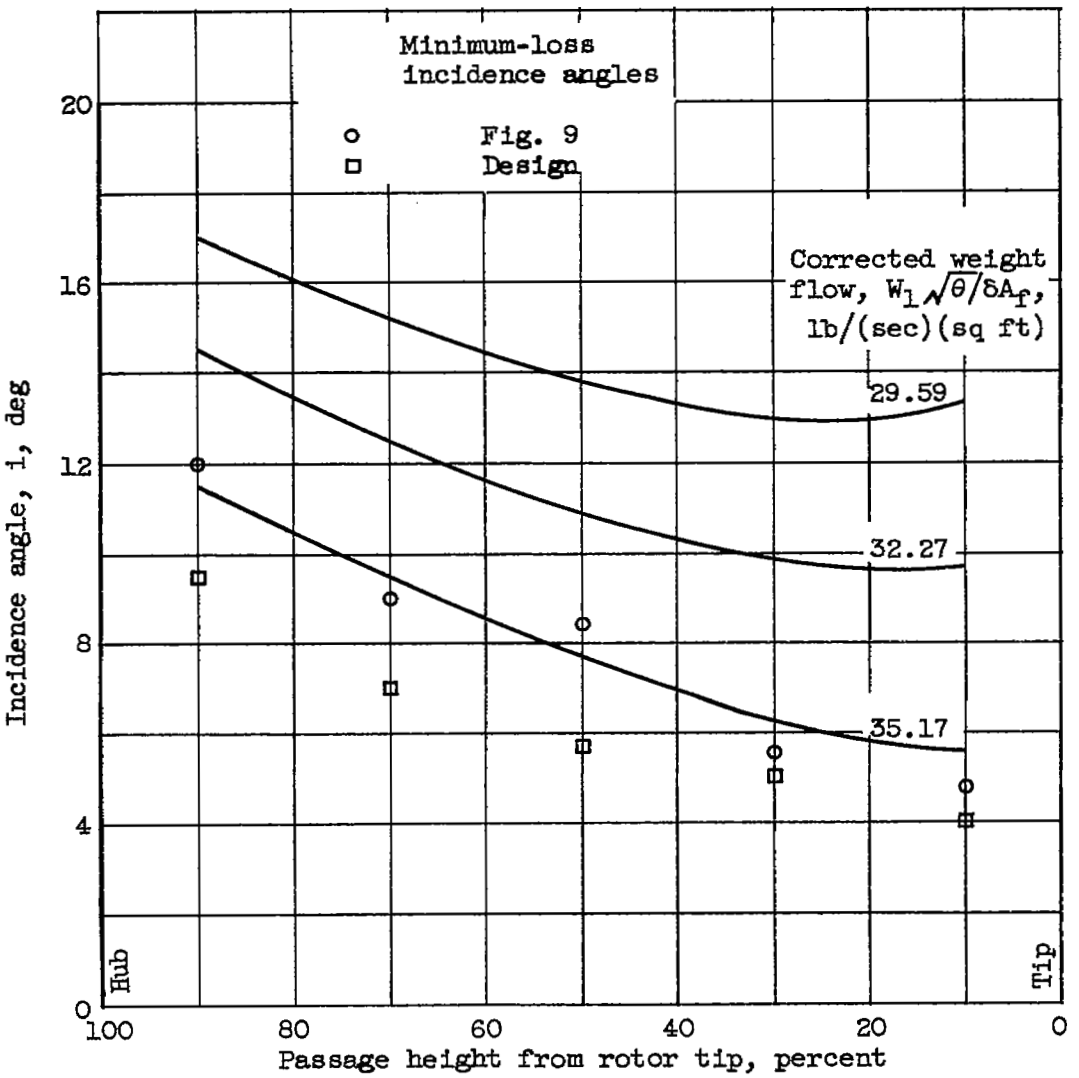

Figure 10. - Incidence-angle variation for reset tapered-tip rotor at design speed.

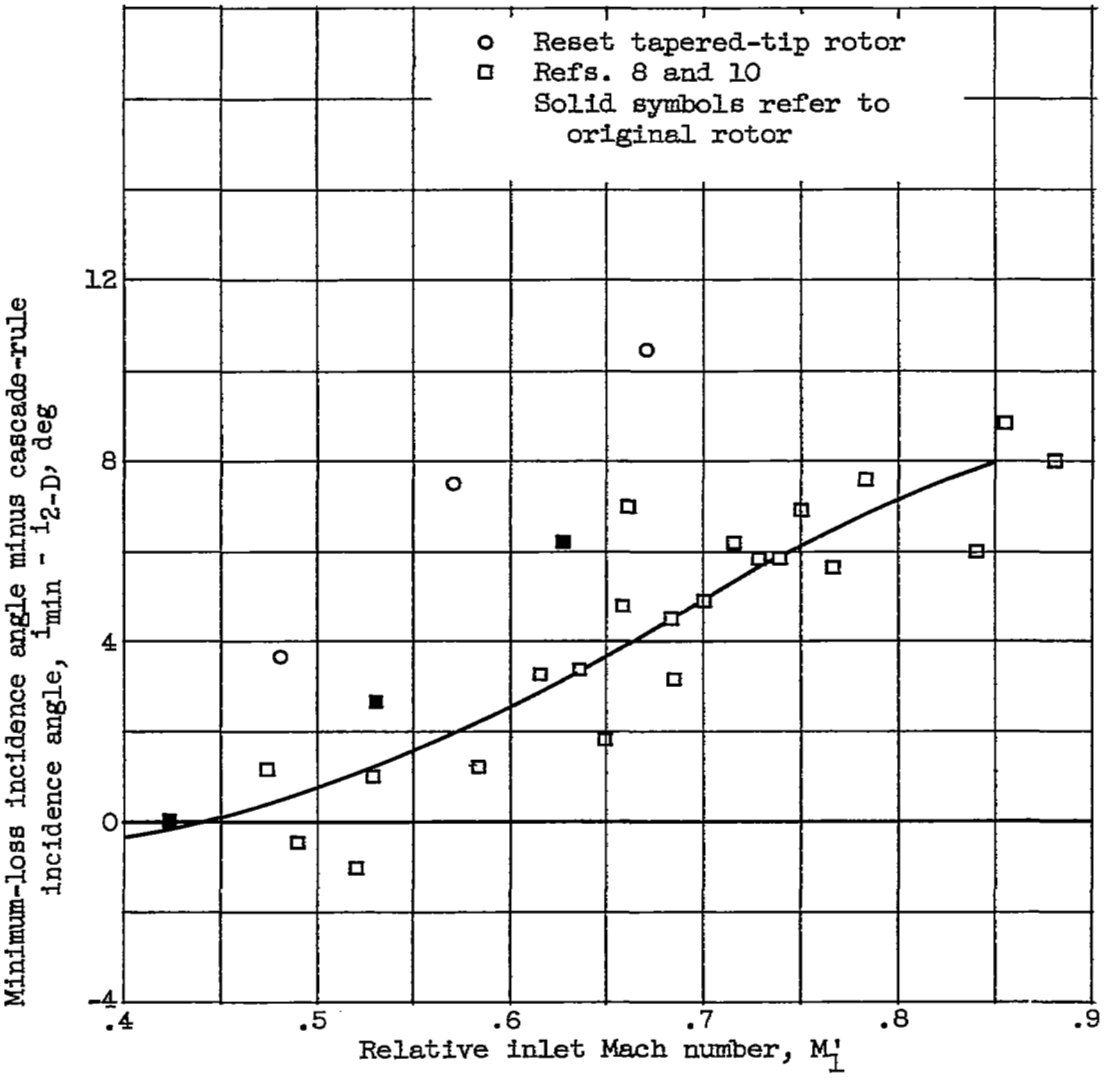

Figure 11. - Variation of minimum-loss incidence angle minus cascade-rule incidence angle with relative inlet Mach number.

[redacted]

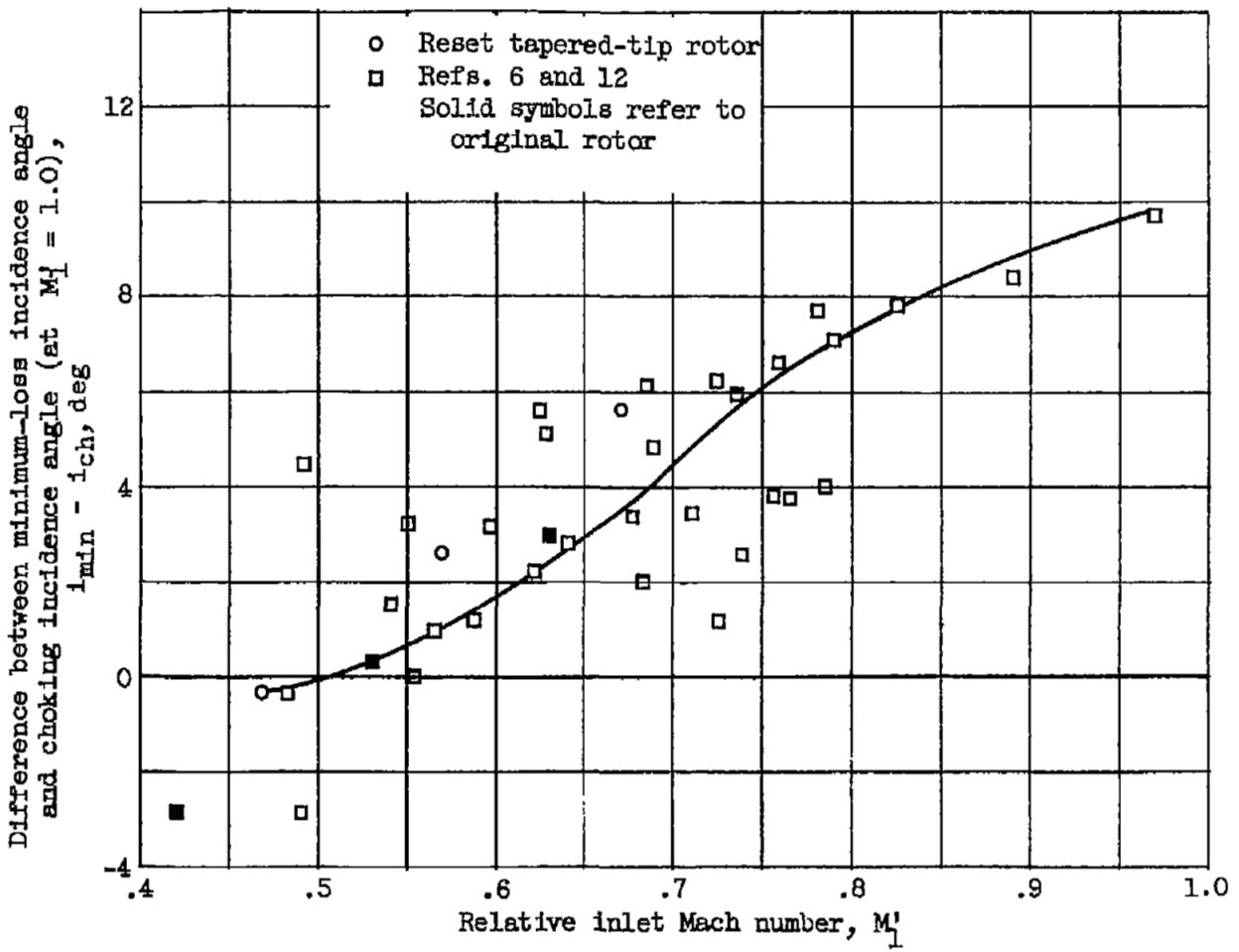

Figure 12. - Variation of minimum-loss incidence angle minus choking incidence angle (at $M_1' = 1.0$) with relative inlet Mach number.